

Comparisons of Two Models for the Simulation of a DC Arc Plasma Torch

Renzhong Huang¹, Hirotaka Fukanuma¹, Yoshihiko Uesugi² and Yasunori Tanaka²
1. Plasma Giken Co., Toshima, Tokyo, Japan, 2. Kanazawa University, Kanazawa City, Japan
*E-mail: RZ_huang@plasma.co.jp

Abstract

The hypothesis of local thermal equilibrium (LTE) in thermal plasma has been widely accepted. Most of the simulation models for the arc plasma torch are based on the hypothesis of LTE and its results indicate a good validity to mimic the pattern of the plasma flow inside the plasma torch. However, due to the LTE hypothesis, the electrical conductivity near the electrodes is significantly low because of the lower gas temperature. Consequently, it is difficult for the flow of electrical current to pass between the anode and cathode. Therefore, a key subject for a model depending on the LTE assumption is to deal with the low electrical conductivity near the electrodes. In this study, two models, determining the electrical conductivity at the vicinity of the electrodes with two different assumptions, were employed to calculate the flow patterns inside a non-transferred DC arc plasma torch. A comparison of the gas temperature, velocity, voltage drop and the heat energy of the plasma arc between the two models were carried out. The results indicate that plasma arc inside the plasma torch fluctuates as simulated by both of the two models. It seems that the model can obtain comparable accuracy compared with the experimental results if the plasma gas electrical conductivity is determined by a nominal electron temperature.

Introduction

Plasma spraying is the injection of metal or ceramic powder into hot gas plasma which melts and projects the molten droplets at high velocity onto a substrate to form coatings. Gas molecules, such as argon or hydrogen, dissociate and recombine, producing an extremely hot, high velocity plasma stream inside a torch (Ref 1). Plasma spraying, one of the most widely used in industrial fields based on thermal plasmas, is commonly employed to provide coatings for protection of materials against wear, erosion, corrosion, and thermal loads. Despite its versatility, the limited reproducibility of the process is a major limitation for its wider application. A major factor for this limited reproducibility is the lack of understanding and control of the dynamic behavior of the arc inside the spraying torch, and the effect of erosion of the anode on the behavior of the plasma jet (Ref 2-6).

A conventional direct-current (DC) non-transferred plasma torch (representing more than 90% of industrial torches) with a stick type cathode is shown schematically in Fig. 1 (Ref 7-8). After the working gas enters the torch, it is heated by an plasma arc formed between a nozzle-shaped anode and a conical cathode, and ejected as a plasma jet. Particles to be sprayed are fed into the particle inlet, heated and accelerated within the plasma jet by the working gas via the plasma arc. The arc inside the torch has been studied experimentally (Ref 4, 6, 9) and numerically (Ref 1-3, 8). Unfortunately, experiments have been limited by the necessity of high cost equipment and lack of understanding of the results obtained.

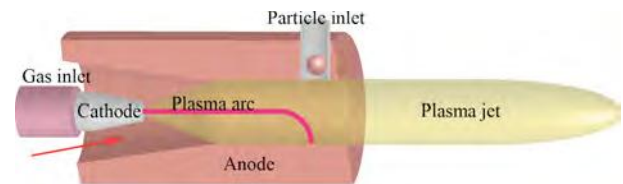


Figure 1: Schematic of a conventional DC plasma spray torch.

Fortunately, numerical calculation provides a valid way to understand the arc behavior inside the plasma torch. The modelling of DC arc plasma torches is an extremely challenging task because the plasma flow is highly nonlinear and presents strong property gradients. It is characterized by a wide range of time and length scales, and often includes chemical and thermodynamic non-equilibrium effects, especially near its boundaries (Ref 8). Despite the complexity of the subject, over the past few decades, many papers concerning numerical studies of the characteristics of DC arc plasma torches have been published (Ref 2-3, 8, 9-22). At the initial stage, a two-dimensional (2D) model was employed in the research to predict the heat transfer and flow patterns inside the plasma torch (Ref 10-14). The predicted arc voltage of the torch in the turbulent regime is much higher than the measured value; in addition the predicted axial location of the arc attachment at the anode surface is also much farther downstream than that observed in experiments (Ref 15). With

Description of the Mathematical Model

Model Assumptions

The two models developed in this study are based on the following main assumptions for simulating the heat transfer and flow patterns inside a plasma torch.

- (1). The continuum assumption is valid and the plasma can be considered as a compressible, perfect gas in local thermal equilibrium state.
- (2). The plasma is optically thin.
- (3). Gravitational effect and viscous dissipation are considered negligible.
- (4). The induced electric field is negligible in comparison with the applied electric field intensity in the plasma arc region.
- (5). The variation of gas pressure inside the torch is so little that the effects of pressure on the thermodynamic and transport properties of plasma are negligible.

According to the forgoing assumption, the thermodynamic and transport properties of the plasma gas, excluding electrical conductivity, are determined by the gas temperature.

Based on the LTE assumption, the value of the electron temperature is equal to the heavy particle temperature, which is low near the electrodes due to the water-cooling, especially near the anode surface. Hence the equilibrium electrical conductivity is extremely low (less than 10^{-2} S/m), which limits the flow of electrical current between the anode and cathode. To alleviate this, two assumptions were employed in this study to mimic the plasma flow inside the plasma torch, and two models were named the improved LTE and conventional LTE model respectively. The improved LTE model is referred to in Ref. 23. In this model, a nominal electron temperature was proposed, that was derived from the plasma gas temperature and adjusted by the electrical field strength, to amend the underestimation of the electrical conductivity caused by the LTE assumption. Therefore, no more additional assumptions are necessary to ensure the electrical current path between the cathode and anode, because the electrical conductivity of plasma gas is determined by the nominal electron temperature instead of the gas temperature. The conventional LTE model is referred to in Ref. 24. In this model, the electrical conductivity is determined basically by the gas temperature. Considering the lower electric conductivity near the cold boundary of the electrode, the vicinity of electrodes (within a distance of 0.1 mm) is artificially considered as a high electrical conductivity of 10^4 S/m, so that a new arc root can be formed if the arc is close enough to the inner surface of the anode.

Governing Equations

Based on the foregoing assumptions, the governing equations for the 3D time-dependent model for the arc plasma can be written as follows:

the rapid development of computer technology, the calculation of heat transfer and fluid flow for a three-dimension (3D) thermal plasma torch with axisymmetrical geometries became feasible (Ref 2-3, 15-22). The models most frequently used for simulations of plasma spray torches rely on the local thermal equilibrium (LTE) approximation, and regard the plasma flow as a property-varying electromagnetic reactive fluid in a state of chemical equilibrium, in which the internal energy of the fluid is characterized by a single gas temperature (Ref 2-3, 15-21). Selvan et al. developed a steady-state 3D LTE model to describe the temperature and velocity distributions inside a DC plasma torch. Moreover the arc length and radius were also discussed. But the model overestimated the local gas temperature near the anodic arc root due to the assumption that all the electric current transferred to the anode only through a fixed arc root (Ref 3, 16). Klinger et al. also developed a steady-state 3D LTE model simulation of the plasma arc inside a DC plasma torch. However, the position of the arc root was determined arbitrarily (Ref 17). With the steady-state 3D LTE models, the temperature and velocity distributions inside a plasma torch, moreover the arc length and power, could be predicted at some level. However, the fluctuation of the plasma arc cannot be determined. Vardelle and Trelles developed a time-dependent 3D LTE model representing the fluctuations of the plasma arc (Ref 2, 18-21). In this unsteady-state 3D LTE model, a critical breakdown electric field or voltage was employed as a criterion to determine the arc root attachment at the anode surface. This made the model more complicated, and it became difficult to calculate. In both the steady- and unsteady-state 3D LTE models, the calculated voltage drop was larger compared with the experimental ones due to the overestimation of electrical resistance with the hypothesis of LTE, especially in the vicinity of the electrodes. In order to mimic the plasma arc more correctly, a non-LTE (NLTE) model was developed for the non-transferred arc plasma torch, which showed better agreement with the experimental results (Ref 22). However, it is extremely difficult to solve the NLTE model because it is necessary to consider the two-temperature chemical equilibrium in comparison with the LTE mode. In our previous studies, an improved time-dependent 3D LTE model was developed and it seems that the results agreed well with the NLTE model, and moreover the experimental results. However, the difference between the improved LTE model and the conventional one has not been clarified yet (Ref 23).

This research is the continuation of Ref 23. In order to differentiate the improved LTE model from the conventional LTE model, the plasma gas temperature and velocity distributions inside a DC plasma torch were calculated using the two different LTE models, and the heat energy of the plasma arc was investigated. The results show that the total voltage drop and the heat energy of the plasma arc obtained by the improved LTE model are more consistent with experimental observations than those of the conventional LTE model.

Conservation of mass:

$$\frac{\partial \rho}{\partial t} + \nabla \cdot (\rho \vec{V}) = 0 \quad (\text{Eq 1})$$

Conservation of momentum:

$$\rho \left(\frac{\partial \vec{V}}{\partial t} + \vec{V} \cdot \nabla \vec{V} \right) = \vec{j} \times \vec{B} - \nabla \left[P + \frac{2}{3} \alpha (\nabla \cdot \vec{V}) \right] + 2 \nabla \cdot (\alpha \vec{S}) \quad (\text{Eq 2})$$

Conservation of energy:

$$\rho c_p \left(\frac{\partial T}{\partial t} + \vec{V} \cdot \nabla T \right) - \frac{DP}{Dt} = \vec{j} \cdot \vec{E} - S_r + \nabla \cdot (\lambda \nabla T) \quad (\text{Eq 3})$$

Maxwell electromagnetism equations:

$$\nabla \cdot (-\sigma \nabla \phi) = 0 \quad (\text{Eq 4})$$

$$\vec{E} = -\nabla \phi \quad (\text{Eq 5})$$

$$\nabla^2 \vec{A} = -\alpha_0 \vec{j} \quad (\text{Eq 6})$$

$$\vec{B} = \nabla \times \vec{A} \quad (\text{Eq 7})$$

Ohm law:

$$\vec{j} = \sigma \vec{E} \quad (\text{Eq 8})$$

Where ρ is gas mass density, t time, \vec{V} velocity, \vec{j} electric current density, \vec{B} magnetic induction vector, P gas pressure, α dynamic viscosity, \vec{S} strain rate tensor, c_p specific heat at constant pressure, T gas temperature, \vec{E} electric field, S_r volumetric net radiation losses, λ gas thermal conductivity, σ electric conductivity, ϕ electric potential, \vec{A} magnetic vector potential and α_0 permeability of free space.

In the improved LTE model, the nominal electron temperature was calculated from the equation as follows (Ref 25):

$$\frac{T_e - T}{T_e} = \frac{3\pi m_h}{32 m_e} \left(\frac{e \lambda_e |E|}{(3/2) k T_e} \right)^2 \quad (\text{Eq 9})$$

Where T_e is the nominal electron temperature, m_h mass of heavy particle, m_e mass of electron, e Elementary charge, λ_e free path of electron.

Computational Domain and Boundary Conditions

The geometry used in the current study corresponds to the SG-100 plasma torch from Praxair. The computational domain formed by the region inside the torch is limited by the cathode, the gas flow inlet, the anode and the outlet as shown in Fig. 2. The computational domain is meshed using 217600 hexahedral cells with 224567 nodes.

As seen in Fig. 2, the boundary of the computational domain is divided into 4 different surfaces to allow the specification of boundary conditions. Table 1 shows the boundary conditions used in the simulation, where P_m represents the inlet pressure equal to 111325 Pa (10 kPa overpressure), h_w the convective heat transfer coefficient at the anode wall equal to $1 \times 10^5 \text{ W.m}^{-2}.\text{K}^{-1}$ (Ref 19-22), T_w a reference cooling water

temperature of 500 K. The current density and temperature of the cathode is defined by:

$$j(r) = J_{cath0} \exp\left(-\left(\frac{r}{R_c}\right)^{n_c}\right) \quad (\text{Eq 10})$$

$$T(r) = 500 + 3000 \exp\left(-\left(\frac{r}{2R_c}\right)^{n_c}\right) \quad (\text{Eq 11})$$

where r is radial distance from the torch axis ($r^2 = x^2 + y^2$), and J_{cath0} and n_c are parameters that specify the shape of the current density profile. The value of R_c is calculated to ensure that the integration of $j(r)$ over the cathode surface equals to the total applied current.

Table 1: Boundary conditions

Boundary	P	V	T	ϕ	A
Inlet	P_m	50 SLM	300 K	$\partial \phi_n = 0$	0
Cathode	$\partial P_n = 0$	0	$T(r)$	$j(r)$	$\partial A_n = 0$
Anode	$\partial P_n = 0$	0	$H_w(T-T_w)$	0	$\partial A_n = 0$
Outlet	1 atm	$\partial V_n = 0$	$\partial T_n = 0$	$\partial \phi_n = 0$	$\partial A_n = 0$

Argon gas was employed as the plasma gas in this study. The spray conditions and the corresponding shape parameters of the cathode current density are shown in Table 2. The thermodynamic and transport properties of the plasma gas are taken from Refs. 26 and 27. For gas flow calculations, the standard K- ϵ model is employed in this study. The governing equations are solved by FLUENT, a commercial computational fluid dynamics (CFD) software developed by Ansys Inc., with the SIMPLE algorithm.

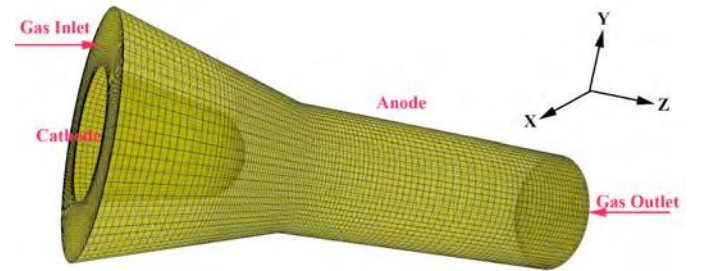


Figure 2: Geometry of the computational domain.

Table 2: Spraying conditions

Current (A)	Flow rate (SLM)	J_{cath0} (A/m ²)	n_c	R_c
400	50	2.0e8	4	0.835093
600	50	2.5e8	4	0.912245

Results and Discussions

Arc Voltage

Figure 3 shows the arc voltages at the applied currents of 400 and 600 A. It can be seen that the arc voltage obtained with the conventional LTE model is much higher than the experimental value owing to the underestimation of the electrical conductivity based on the LTE assumption. The arc voltage obtained with the conventional LTE model fluctuates

with the amplitude between 52 and 56 V for electrical current of 400 A and between 48 and 52 V for the applied current of 600 A. The arc voltage calculated by the improved LTE model is more consistent with the experimental value and fluctuates only for the applied current of 600 A as shown in Fig. 3. However, the arc voltage calculated with the improved LTE model is a little lower than the experimental value. This situation is caused by the sheath voltage of the cathode, which is not considered in the current study. According to the studies of Benilov and Zhou, higher electrode temperature and electric current density lead to a lower sheath voltage drop (Ref 28-29). Therefore, the experimental arc voltage decreased with the increase of applied current, and the calculated arc voltage obtained with the improved LTE model became closer to the experimental value with the increase of the applied current.

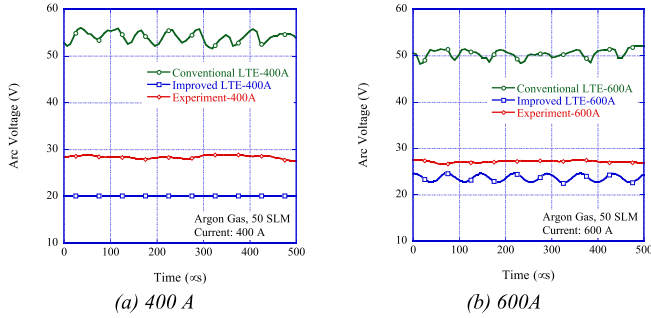


Figure 3: The time-evolution of arc voltage.

Gas Temperature and Velocity Inside the Torch

Figure 4 shows the instantaneous gas temperature distributions inside the plasma torch calculated by the two LTE models at several representative times for observing the conditions of arc voltage. It reveals that the gas temperature inside the plasma torch fluctuates with the elapse of time at the applied currents of both 400 and 600 A (see Figs. 4a and 4b) calculated by the conventional LTE model, and slightly fluctuates only at the applied current of 600 A (see Fig. 4d) calculated by the improved LTE model. The plasma gas temperature inside the torch increased with the increase of the applied current regardless of which model was used owing to the increase of input electrical energy. Although the distributions of the gas temperature calculated by the two models are somewhat different, the similar scale of the temperature inside the torch was obtained.

Figure 5 shows the instantaneous gas velocity distributions inside the plasma torch calculated by the two LTE models at the applied currents of 400 and 600 A. Similar to the gas temperature distributions, the gas velocity fluctuates for both the applied currents of 400 and 600 A (see Figs. 5a and 5b) calculated by the conventional LTE model, and for only the applied current of 600 A (see Fig. 5d) calculated by the improved LTE model. The gas velocity inside the plasma torch increased with the increase of applied current for both of the two LTE models. The gas velocity calculated by the conventional LTE model is a little higher than the one calculated by the improved LTE model.

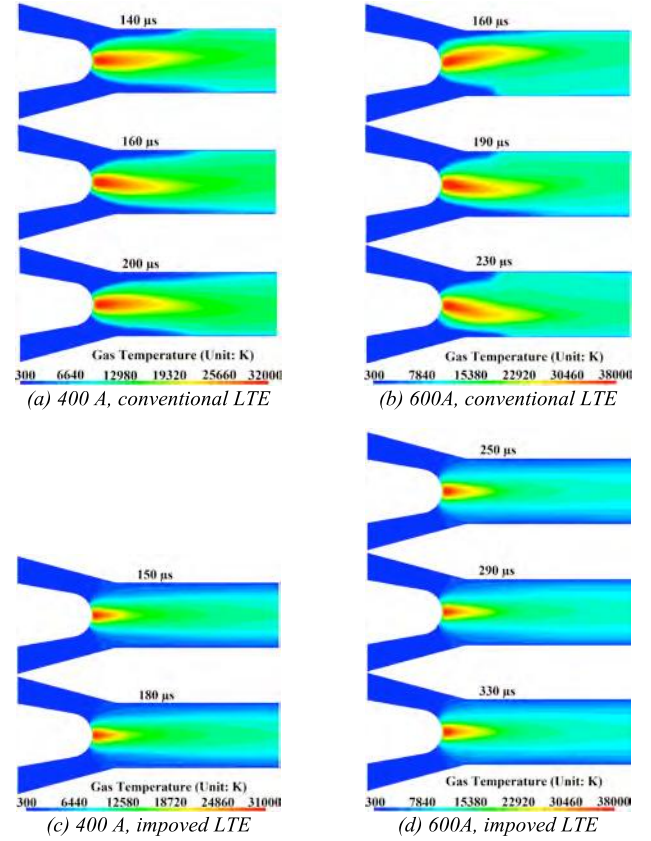


Figure 4: Gas temperature distributions inside the torch.

Gas Temperature and Velocity at the Torch Exit

Figures 6 and 7 show the gas temperature and velocity distributions at the torch exit calculated by the two LTE models respectively. It can be seen that the gas temperature and velocity at the torch exit increased with the increase of the applied current for both of the two LTE models owing to the increase of the input electrical energy. The gas temperature and velocity at the torch exit calculated by the conventional LTE model are higher than the ones calculated by the improved LTE model.

Heat Energy of the Plasma Arc

In order to estimate the accuracy of the two LTE models, the heat energy of the plasma arc was measured. The total heat transferred to the plasma arc from the electric energy is calculated by

$$Q_{plasma} = U_p I - \rho_w F_w C_{wp} (T_2 - T_1) \quad (\text{Eq 12})$$

where U_p is the voltage between the two electrical cables where the cooling water temperature was measured, I the applied current, ρ_w the density of, F_w the flow rate of, and C_{wp} the specific heat of the cooling water. T_1 and T_2 represent the cooling water temperatures at the inlet and outlet inside the electric cables.

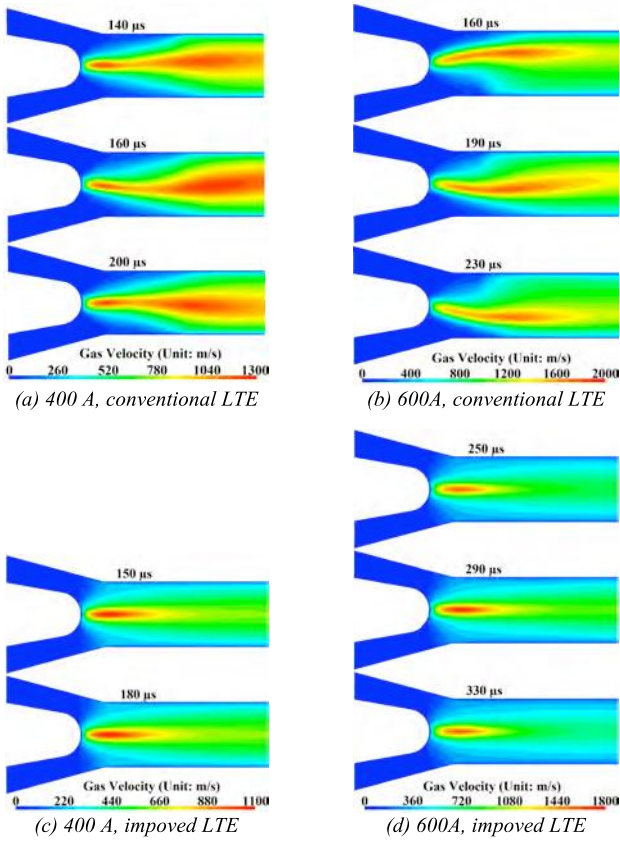


Figure 5: Gas velocity distributions inside the torch

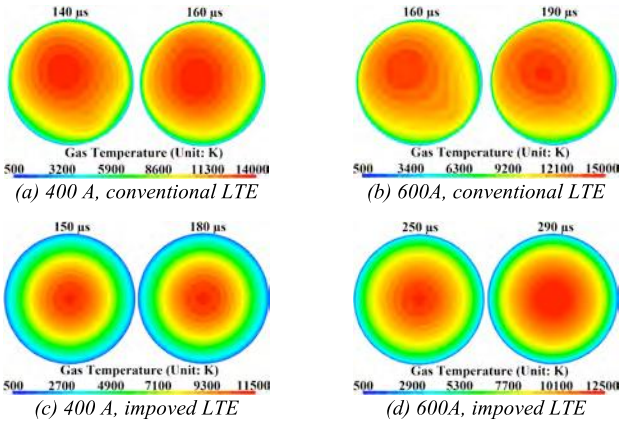


Figure 6: Gas temperature distributions at the torch exit.

The amount of heat transferred to the plasma in the numerical calculation can be calculated by the integration of the gas heat enthalpy through the plane of the torch exit. It can be described as

$$Q_{plasma} = \iint c_p m_f (T - T_0) ds \quad (\text{Eq 13})$$

where c_p is the specific heat of the gas, m_f the mass flow rate of the gas, T the gas temperature, T_0 the initial gas temperature at the nozzle inlet, and s the area of the plane of torch exit.

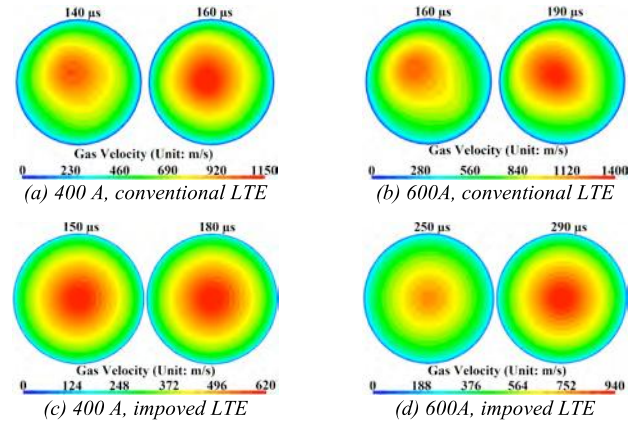


Figure 7: Gas velocity distributions at the torch exit.

The average heat energy of the plasma arc calculated and measured are shown in Fig. 8. It can be seen that the average heat energy of the plasma arc calculated by the conventional LTE model is much higher than that of the experiment, and the average heat energy of the plasma arc calculated by the improved LTE model is nearly identical with the experimental one. It seems that the improved LTE model can obtain a high accuracy compared with the conventional model.

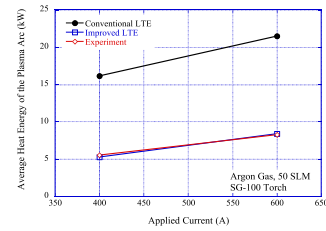


Figure 8: Average heat energy of the plasma arc.

Conclusions

In this study, two LTE models had been developed and applied to the three-dimensional and time-dependent simulation of the flow inside a DC arc plasma torch. The temperature and velocity distributions of arc gas inside the torch were calculated, and the gas flow fluctuated with the elapse of time. Compared with the results calculated by the two different models, it can be seen that the gas temperature and velocity inside the torch obtained with the conventional LTE model are a little higher than the values obtained with the improved LTE model owing to the underestimation of the electrical conductivity. The arc voltage and the heat energy of the arc calculated by the improved LTE model agree more with the experimental results than the results obtained with the conventional LTE model.

References

1. G. V. Miloshevsky, G. S. Romanov, V. I. Tolkach and I. Yu. Smurov, Simulation of the Dynamics of Two-Phase Plasma Jet in the Atmosphere. *Proceedings of III International Conference on Plasma Physics and Plasma*

- Technology, Minsk, Belarus, September 18-22, 2000, p 244-247
2. Juan Pablo Trelles, Emil Pfender and Joachim Heberlein, Multiscale Finite Element Modeling of Arc Dynamics in a DC Plasma Torch, *Plasma Chemistry and Plasma Processing*, 2006, 26(6), p 557-575
 3. B. Selvan and K. Ramachandran, Comparisons Between Two Different Three-Dimensional Arc Plasma Torch Simulations, *J. Therm. Spray Technol.*, 2006, 18(5-6), p 846-857
 4. Z. Duan and J. Heberlein, Arc Instabilities in a Plasma Spray Torch, *J. Therm. Spray Technol.*, 2002, 11(1), p 44-51
 5. D. Outcalt, M. Hallberg, G. Yang, J. Heberlein, E. Pfender and P. Strykowski, Instabilities in Plasma Spray Jets, *Thermal Spray 2006: Science, Innovation, and Application* (ASM International), (Ed.) Basil R. Marple, Margaret M. Hyland, Yuk-Chiu Lau, Rogerio S. Lima and Joel Voyer, May 15-18, 2006, Seattle, Washington, p 803-807
 6. J. F. Coudert, M. P. Planche and P. Fauchais, Characterization of DC Plasma Torch Voltage Fluctuations, *Plasma Chemistry and Plasma Processing*, 1996, 16(1), p 211S-227S
 7. P. Fauchais, Understanding Plasma Spraying, *J. Phys. D: Appl. Phys.*, 2004, 37(9), R86-R108
 8. J.P. Trelles, C. Chazelas, A. Vardelle, and J.V.R. Heberlein, Arc Plasma Torch Modeling, *J. Therm. Spray Technol.*, 2009, 18(5-6), p 728-752
 9. R. Ramasamy and V. Selvarajan, Current-Voltage Characteristics of a Non-Transferred Plasma Spray Torch, *The European Physical Journal D*, 2000, 8(1), p 125-129
 10. R. Westhoff, A. H. Dilawari and J. Szekely, A Mathematical Representation of Transport Phenomena Inside a Plasma Torch, *Mats. Res. Soc. Sym. Proc.*, 1991, 199, p 213-219
 11. R. Westhoff and J. Szekely, A Model of Fluid, Heat Flow, and Electromagnetic Phenomena In a Nontransferred Arc Plasma Torch, *J. of Appl. Phys.*, 1991, 70(7), p 3455-3466
 12. Han Peng, Yu Lan and Chen Xi, Modeling of Plasma Jets with Computed Inlet Profiles, *Proceedings of the 13th International Symposium on Plasma Chemistry*, C.K. Wu, Ed., Peking University Press, Beijing, 1997, p 338-343
 13. D. A. Scott, P. Kovitya, G. N. Haddad, Temperatures in the Plume of a DC Plasma Torch, *J. of Appl. Phys.*, 1989, 66(11), p 5232-5239
 14. Seungho Paik, P. C. Huang, J. Heberlein, and E. Pfender, Determination of the Arc Root Position in a DC Plasma Torch, *Plasma Chemistry and Plasma Processing*, 1993, 13(3), p 379-397
 15. He-Ping Li and E. Pfender, Three Dimensional Modeling of the Plasma Spray Process, *J. Therm. Spray Technol.*, 2007, 16(2), p 245-260
 16. B. Selvan, K. Ramachandran, K. P. Sreekumar, T. K. Thiyagarajan and P. V. Ananthapadmanabhan, Three-Dimensional Numerical Modeling of an Ar-N₂ Plasma Arc Inside a Non-Transferred Torch, *Plasma Science and Technology*, 2009, 11(6), p 679-687
 17. L. Klinger, J.B. Vos, K. Appert, High-Resolution CFD Simulation of a Plasma Torch in 3 Dimensions, CRPP-REPORT-2003-024, LRP 762, http://infoscience.epfl.ch/record/121307/files/lrp_762_03_hq.pdf (2003)
 18. C. Baudry, A. Vardelle, G. Mariaux, F. C. Delalondre and F. E. Meillot, Three-Dimensional and Time-Dependent Model of the Dynamic Behavior of the Arc in a Plasma Spray Torch, *Thermal Spray 2004: Advances in Technology and Applications* (ASM International), (Ed.) D. von Hofe, May 10-12, 2004 (Osaka, Japan), p717 - 723 (2004)
 19. E. Moreau, C. Chazelas, G. Mariaux and A. Vardelle, Modeling the Restrike Mode Operation of a DC Plasma Spray Torch, *J. Therm. Spray Technol.*, 2006, 15(4), p 524-530
 20. J. P. Trelles, E. Pfender and J. V. R. Heberlein, Modelling of the Arc Reattachment Process in Plasma Torches, *Journal of Physics D: Applied Physics*, 2007, 40(18), p 5635-5648
 21. J. P. Trelles and J. V. R. Heberlein, Simulation Results of Arc Behavior in Different Plasma Spray Torches, *J. Therm. Spray Technol.*, 2006, 15(4), p 563-569
 22. J. P. Trelles, J. V. R. Heberlein and E. Pfender, Non-equilibrium Modelling of Arc Plasma Torches, *J. Phys. D Appl. Phys.*, 2007, 40(19), p 5937-5952
 23. R. Huang, H. Fukanuma, Y. Uesugi, Y. Tanaka, An Improved Local Thermal Equilibrium Model of DC Arc Plasma Torch; *IEEE T. Plasma Sci.*, 2011, 39(10), p 1974-1982
 24. R. Huang, H. Fukanuma, Y. Uesugi, Y. Tanaka; Simulation of Arc Root Fluctuation in a DC Non-transferred Plasma Torch with Three Dimensional Modeling; *International Thermal Spray Conference and Exposition (ITSC 2011)*; September 27 - 29, 2011; CCH - Congress Center Hamburg/Germany; p1278-1283 (2011)
 25. M. F. Zhukov and I. M. Zasytkin, *Thermal Plasma Torches: Design, Characteristics, Application*, Cambridge International Science Publishing, 2007, p3
 26. M. I. Boulos and P. Fauchais, *Thermal Plasmas: Fundamentals and Applications*, Vol I, Publisher: Springer, 1994
 27. V. Colombo, E. Ghedini and P. Sanibondi, Thermodynamic and Transport Properties in Non-Equilibrium Argon, Oxygen and Nitrogen Thermal Plasmas, *Progress in Nuclear Energy*, 2008, 50(8), p 921-933
 28. M. S. Benilov, Understanding and Modelling Plasma-Electrode Interaction in High-Pressure Arc Discharges: A Review, *J. Phys. D: Appl. Phys.* 41 (2008), p1-30
 29. X Zhou and J Heberlein, Analysis of the Arc-Cathode Interaction of Free-Burning Arcs, *Plasma Source Sci. Technol.* 3 (1994), p564-574